3D INSIGHTS

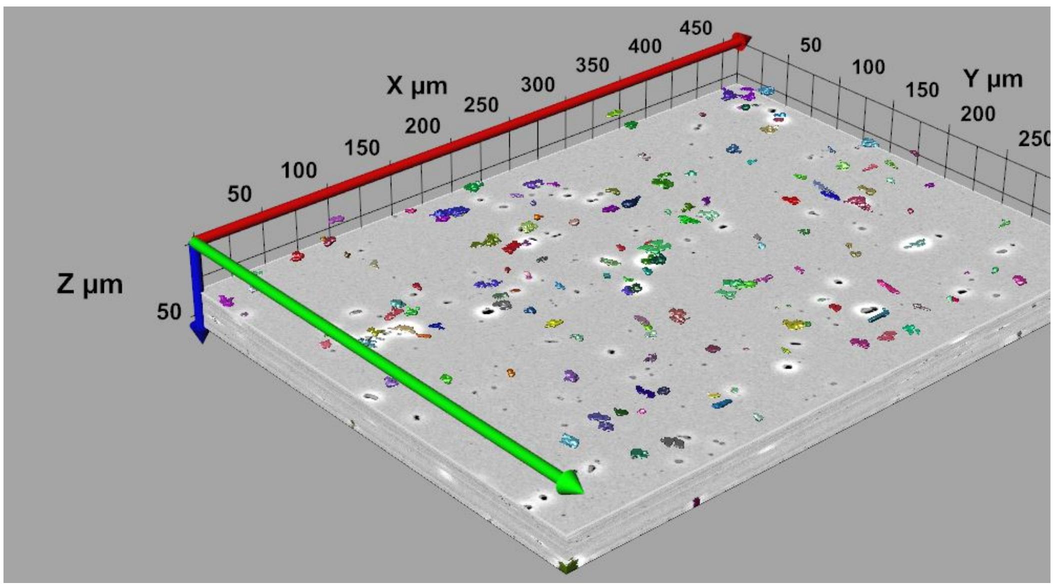

Oct 2017

3D Characterization of AlFeSi Intermetallics in a 6xxx Series Al Alloy using Robo-Met.3D

We analyzed the volume percentage of intermetallic phase (AlFeSi) content in an aluminum alloy using automated 3D metallography. The presence of intermetallic phases, can impair the deformability of extrudable 6xxx series alloys. The Robo-Met.3D® system revealed the desired features in the sample. Post processing segmentation was used to quantify the intermetallic phase distribution.

3D Characterization of AlFeSi Intermetallics in a 6xxx Series Al Alloy using Robo-Met.3D

MATERIAL BACKGROUND

In this application note we describe serial sectioning analysis to evaluate intermetallic phases (AlFeSi) in an aluminum alloy. Extrudable Al-alloys of the 6xxx series are typically fabricated using direct-chill casting followed by a homogenization cycle, prior to hot extrusion. As-cast billets contain several inhomogeneities, including iron intermetallics[i]. While iron-rich intermetallics can reduce die soldering in high pressure die casting, some intermetallic phases, particularly β-AlFeSi with plate-like morphology, have a deleterious effect on mechanical properties[ii]. The morphology of these intermetallics can limit extrudability by inducing local cracking and surface defects in extruded parts. In contrast, α-AlFeSi intermetallics feature more equiaxed, or spherical morphology[iii].

The analysis of intermetallics distribution is therefore of interest. Accurate characterization of intermetallic phases plays a central role to analyze properties of aluminum alloys.· Al 6xxx alloys have widespread application in aircraft and automotive industry segments[iv]· Developing a more thorough understanding of intermetallic phase content is important in generating an accurate predictive model[v].

SERIAL SECTIONING ANALYSIS USING ROBO-MET.3D®

Robo-Met.3D is a fully automated serial sectioning system that generates microstructural data for three dimensional reconstructions and analysis. Common applications of Robo-Met.3D include studying additively manufactured components[vi], analysis of welds and thermal barrier coatings[vii], and fiber orientation effects in ceramic matrix composites[viii].

For this study, an Aluminum alloy sample of proprietary composition was provided to UES for analysis of intermetallic features such as AlFeSi. Optical images were automatically acquired with the microscope built into the Robo-Met.3D system, at a magnification of 500X. The resultant spatial resolution was 0.21 microns along X and Y axes. Less than a millimeter of z-dimension was analyzed (approx. 60.0 microns) in 112 sections or slices at an average slice thickness of 0.52 microns. Each slice contained a montage of 2 X 2 images, for an image size of approximately 500 microns along x and 400 microns y axes.

IMAGE PROCESSING PARAMETERS

The 2D image tiles from each layer were stitched into montages (or mosaics) and then registered with the images from the next layer using Fiji and Image J software. 3D analysis was performed using Image-Pro Premier 3D v.9.3. For 3D analysis, the loaded z-stack of 112 sections was processed with subsampling along X, Y and Z directions. A 3D isosurface was created without any filtering to extract the volume distribution of the intermetallic phase (Fig. 3).

An image histogram was used to threshold the intermetallic phase. Based on intensity values, the range for the intermetallic phase is set to 0-128. For quantification, size threshold feature was set to 3 microns along width, height, and depth; and volume parameters were extracted. The segmented images were analyzed using routines built into Image-Pro.

IMAGING RESULTS

Figure 1 illustrates the raw 2D image. Figure 2, in contrast, illustrates the combined stack of 112 slice images. The intermetallic phases are clearly visible along with some porosity induced in processing.

Fig. 1: Raw 2D Image

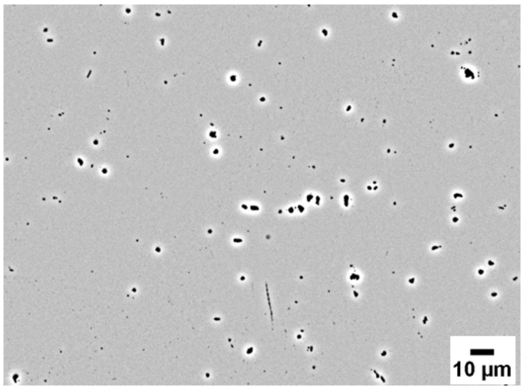

Fig. 2: 3D Image (stack of 112 slices)

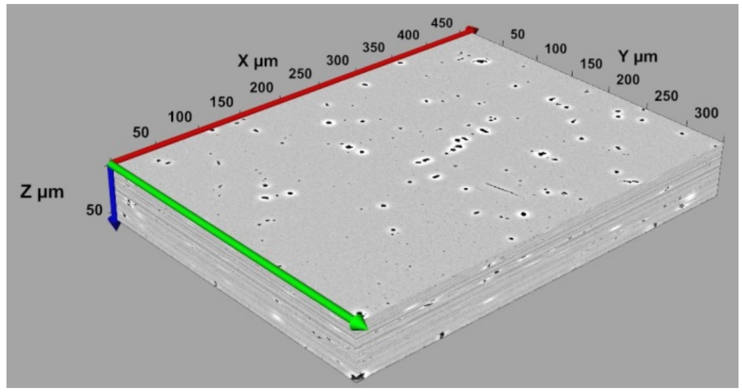

POST-PROCESSING RESULTS

Figure 3 illustrates the segmented intermetallic phases and their distribution in the 500x400x400 micron volume analyzed.

Fig. 3: 3D Intermetallic Phase Distribution

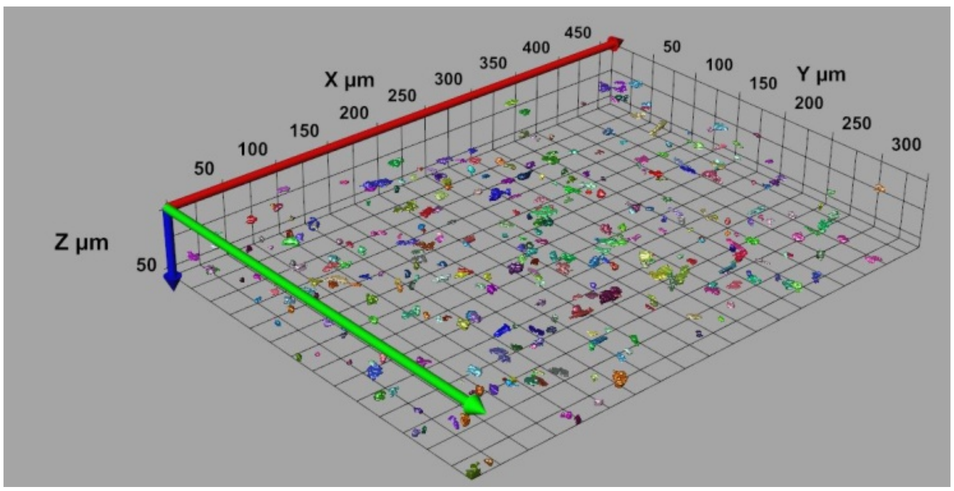

Each feature was identified with specific index value based on size. The volume percentage of the intermetallic phase was less than 1.0 vol %. The equiaxed morphology suggests predominantly α-AlFeSi intermetallics.

It is useful to compare the current 2D methods, where a specific feature of interest is extrapolated from a single slice, to the complete 3D volume description. In order to do this, about 10 sections spaced through the analysis volume were selected. The variation in the feature size (AlFeSi) measure calculated from each 2D slice is significant, ranging from ~ 9-21 microns, as illustrated in Fig. 4. By contrast, the 3D equivalent spherical diameter is calculated as about 11 microns.

Hence, visualization of the 3D topological features using serial sectioning methods such as Robo-Met.3D creates a better understanding of the actual microstructural features compared to using the estimations such as surface area and volume fraction from classical stereological methods.

Fig. 4: Variations in 2D Analysis of Intermetallics Feature Dimensions

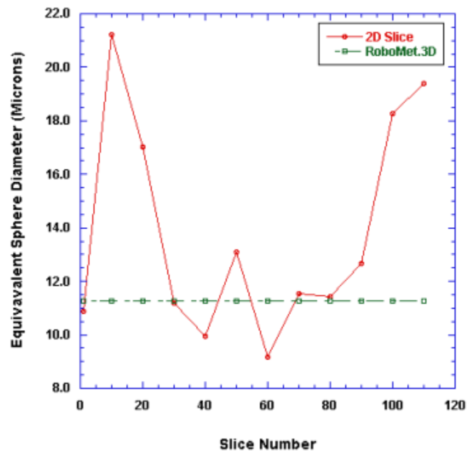

CONCLUSIONS

The study successfully demonstrates the use of RoboMet.3D in automated metallography. The system proved capable of collecting image data with high fidelity, and controlled slice thicknesses, in an automated manner. The resultant dataset was useful in visualization and analysis of the AlFeSi intermetallics in an Al6xxx alloy sample.

CONTRIBUTORS

Bryan Turner and Satya Ganti (UES) performed the image collection and post-processing. Animated views of the data are available at www.ues.com.

REFERENCES

[i] Sarafoglou, P. I., Aristeidakis, J. S., Tzini, M. I. T., & Haidemenopoulos, G. N. (2016). Metallographic Index-Based Quantification of the Homogenization State in Extrudable Aluminum Alloys. Metals, 6(5), 121.
[ii] Ji, S., Yang, W., Gao, F., Watson, D., & Fan, Z. (2013). Effect of iron on the microstructure and mechanical property of Al–Mg–Si–Mn and Al–Mg–Si diecast alloys. Materials Science and Engineering: A, 564, 130-139.
[iii] Taylor, J. A. (2012). Iron-containing intermetallic phases in Al-Si based casting alloys. Procedia Materials Science, 1, 19-33.
[iv] G. Mrowka-Nowotnik, J. Sieniawski, M. Wierzbinska (2007). Intermetallic phase particles in 6082 aluminium alloy. Archives of Materials Science and Engineering, 2, 69-76.
[v] M. Rosefort, C. Matthies, H. Buck, H. Koch. Determination of a- and b-AlFeSi-Phases in Wrought Aluminium Alloys. TRIMET ALUMINIUM AG.
[vi] Seifi, M., Ghamarian, I., Samimi, P., Collins, P. C., & Lewandowski, J. J. (2016). Microstructure and mechanical properties of Ti-48Al-2Cr-2Nb manufactured via electron beam melting. In *Ti-2015: The 13th World Conference on Titanium*.
[vii] Madison, J. D., Huffman, E. M., Poulter, G. A., & Kilgo, A. C. (2015). *R3D at Sandia National Laboratories-A User Update* (No. SAND2015-7665PE). Sandia National Laboratories (SNL-NM), Albuquerque, NM (United States).
[viii] Bricker, S., Simmons, J. P., Przybyla, C., & Hardie, R. (2015, March). Anomaly detection of microstructural defects in continuous fiber reinforced composites. In *SPIE/IS&T Electronic Imaging* (pp. 94010A-94010A). International Society for Optics and Photonics.